This article has been accepted for inclusion in a future issue of this journal. Content is final as presented, with the exception of pagination.



# Impact of Air Temperature Inversion on the Clear-Sky Surface Downward Longwave Radiation Estimation

Jie Cheng, *Senior Member, IEEE*, Shunlin Liang, *Fellow, IEEE*, and Jiancheng Shi, *Fellow, IEEE*

***Abstract*— Parameterization schemes for estimating clear-sky surface downward longwave radiation (SDLR) are well recognized for their simplicity and acceptable accuracy, especially at the local scale. The near-surface temperature and/or water vapor are usually used to predict the clear-sky SDLR in a parameterization scheme. Air temperature inversion (ATI) alters the atmospheric state at the near-surface boundary layer and affects the accuracy of the clear-sky SDLR estimation. However, few studies have investigated the impact of ATI on the estimate of the clear-sky SDLR. This article investigated the impact of ATI on the estimate of the clear-sky SDLR using six widely used parameterization schemes. According to the evaluation results using ATI profiles from the Thermodynamic Initial Guess Retrieval (TIGR) database and the Surface Radiation Budget Network (SURFRAD) sites, all the parameterization schemes are sensitive to ATI, and their accuracy is degraded greatly as a whole. The SDLR is underestimated for the ATI profile both in the TIGR database and SURFRAD sites. The best three schemes can achieve the accuracy with bias values of approximately −10 W/m$^2$ and root-mean-square errors (RMSEs) less than 20 W/m$^2$ for the ATI profiles in the TIGR database. The reason the SDLR is underestimated for the ATI profiles is provided by a simulation study. An empirical method is proposed to correct the impact of ATI. The accuracy of all the parameterization schemes is remarkably improved at SURFRAD sites after correcting the impact of ATI, with the absolute values of bias and RMSEs less than 10 and 20 W/m$^2$ at SURFRAD sites.**

***Index Terms*— Air temperature inversion (ATI), parameterization scheme, SRB network (SURFRAD), surface downward longwave radiation (SDLR), surface radiation budget (SRB).**

## I. Introduction

The surface downward longwave radiation (SDLR, 4–100 $\mu$m) is one of the four components required to calculate the Earth's surface radiation budget (SRB), which regulates land surface processes such as evapotranspiration and oceanic and atmospheric circulations [1]–[3]. The clear-sky SDLR is determined by the vertical profiles of the atmospheric temperature, moisture, and other gases [4], [5]. The SDLR is dominated by the radiation of a shallow layer close to the surface [6]. For example, the lowest 10 m layer of the atmosphere contributes 32%–36% of the total SDLR, whereas the atmosphere above 500 m from the surface accounts for only 16%–20% of the total SDLR. Therefore, the near-surface temperature and/or water vapor are used to predict the SDLR based on the Stefan–Boltzmann equation

$$\mathrm{SDLR} = \varepsilon(T_\mathrm{a}, e_\mathrm{a})\sigma T_\mathrm{a}^4 \tag{1}$$

where $\sigma$ is the Stefan–Boltzmann's constant ($5.67 \times 10^{-8}$ W m$^{-2}$ K$^{-4}$). $\varepsilon$ is the atmospheric effective emissivity under clear-sky conditions and can be formulated as a function of the air temperature ($T_\mathrm{a}$), water vapor pressure ($e_\mathrm{a}$), or both at the screen level. Equation (1) is also known as the parameterization scheme. Different strategies have been employed to represent $\varepsilon$ under clear-sky conditions, and various parameterization schemes have been formed [5], [7]–[14]. The parameterization scheme is usually site-specific [15]. Their performance is primarily affected by geographical locations and local environmental conditions [16], [17]. The parameterization scheme can achieve a high SDLR estimation accuracy if it is adjusted or calibrated by local observational data and can achieve a more robust estimate under various environmental conditions when integrating the parameterization schemes with better performance by Bayesian model averaging (BMA) [16]–[18]. Therefore, the parameterization scheme has gained popularity in estimating the SDLR at the local scale.

Air temperature inversion (ATI) usually occurs at the near-surface boundary layer, especially in mountainous regions [19] and the Antarctic Plateau [20]. Previous studies have demonstrated that ATI induces extra errors in the retrieval of the land surface temperature (LST) and sea surface temperature (SST) [21], [22]. Tang *et al.* [19] incorporated the ATI profiles from the Thermodynamic Initial Guess Retrieval (TIGR) database [23] into the generalized split-window (GSW) algorithm [24] and improved the LST retrieval accuracy under ATI conditions. According to the sensitivity study of Gupta [25], 86% of the SDLR comes from the first layer of the atmosphere, which is 50 hPa thick. The occurrence of ATI in the near-surface boundary layer alters the atmospheric state and certainly affects the estimate of the SDLR using a parameterization scheme that does not consider the ATI phenomenon.

Manuscript received October 5, 2019; revised November 25, 2019; accepted January 11, 2020. This work was supported in part by the Second Tibetan Plateau Scientific Expedition and Research Program (STEP) under Grant 2019QZKK0206, in part by the National Natural Science Foundation of China under Grant 41331173, and in part by the National Key Research and Development Program of China under Grant 2016YFA0600101. *(Corresponding author: Jie Cheng.)*

Jie Cheng and Jiancheng Shi are with the State Key Laboratory of Remote Sensing Science, Jointly Sponsored by the Beijing Normal University and the Institute of Remote Sensing and Digital Earth, Chinese Academy of Sciences, Beijing 100875, China (e-mail: jie_cheng@bnu.edu.cn).

Shunlin Liang is with the Department of Geographical Science, University of Maryland, College Park, MD 20742 USA.

Color versions of one or more of the figures in this article are available online at http://ieeexplore.ieee.org.

Digital Object Identifier 10.1109/TGRS.2020.2967432

To our knowledge, the sensitivity and applicability of parameterization schemes for clear-sky SDLR estimates have rarely been investigated under ATI conditions. The objective of this article is to investigate the sensitivity and applicability of the widely used parameterization schemes to ATI and provide guidance on how to select a suitable parameterization scheme and correct the impact of ATI when estimating the clear-sky SDLR under ATI. Section II describes the data and methods used to investigate the impact of ATI. Section III provides the estimation results of clear-sky SDLR under ATI using simulated and observational data. The reason the SDLR is underestimated for the ATI profiles and an empirical method for correcting the impact of ATI are presented in Section IV, and Section V provides a short summary.

## II. Data and Methods

### A. Data

*1) TIGR Database:* The latest TIGR data set is a climatological library of 2311 representative atmospheric situations selected using statistical methods from 80 000 radiosonde reports [23], [26]. Each atmospheric situation is described by the temperature and the water vapor and ozone concentrations at 40 levels between 0.05 and 1013 hPa. The water vapor content of TIGR varies from 0.1 to 8.0 g/cm$^2$, and the bottom-level temperature ranges from 231 to 315 K. The TIGR database has been widely applied in algorithm development for the retrieval of the LST and surface upwelling longwave radiation for its representativeness [27]–[30]. The clear-sky ATI profiles in the TIGR database were used to investigate the impact of ATI on the estimate of the clear-sky SDLR.

*2) SURFRAD:* The SRB network (SURFRAD) was established in 1993 by the National Oceanic and Atmospheric Administration's Office of Global Programs [31]. SURFRAD provides the measurements of the SRB components (including upwelling and downward solar and infrared radiation and direct and diffuse solar radiation) and meteorological parameters over seven sites that cover the grassland, cropland, and desert land cover types. SURFRAD measurements have been widely used for the validation of satellite-derived land surface and atmospheric products. The SDLR was measured by the Precision Infrared Radiometers (model PIR, Eppley Laboratories, Newport, RI, USA) in the spectral range of 3–50 $\mu$m; this instrument can cover the spectral range of 4–100 $\mu$m via calibration. The PIRs are mounted ~8 m above the ground, and the maximum signal comes from a 45° viewing zenith angle. The overall accuracy of the measured data is approximately ±9 W/m$^2$ [31]. The SDLR measurements are averaged every 3 min and distributed in near real-time by anonymous FTP (http://www.srrb.noaa.gov). Three years (2003–2005) of measurements at seven SURFRAD sites were downloaded and used in this article.

*3) MODIS Atmospheric Profile Product:* The Moderate Resolution Imaging Spectroradiometer (MODIS) atmospheric profile product (MOD07/MYD07) is produced by the MODIS Atmosphere Science Team [32]. It contains the temperature, dew point, and geopotential height profiles estimated at 20 fixed pressure levels ranging from 5 to 1000 hPa. MOD07/MYD07 also provides the surface pressure and elevation. The spatial resolution of MOD07/MYD07 is 5 km at nadir. Three years (2003–2005) of data collocated with the SURFRAD sites were downloaded and used to identify the occurrence of ATI at the SURFRAD sites.

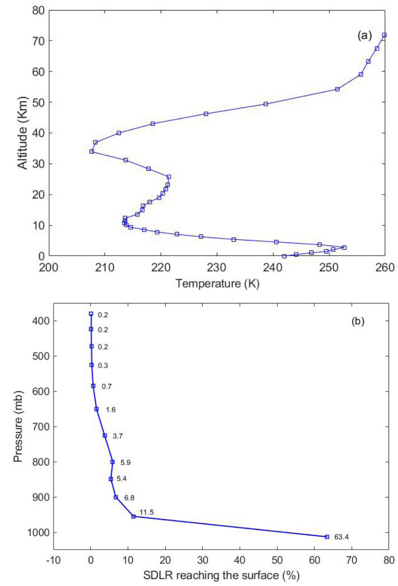


Fig. 1. (a) Example of the ATI profile from the TIGR database. (b) Contribution of each layer to the total SDLR.

### B. ATI Profile Identification

If the temperature difference between the second level and bottom level (i.e., the surface) is larger than 1 K, then ATI occurs, and the atmospheric profile is identified as an ATI profile [Fig. 1(a)]. The 1 K threshold was used for the consideration of the errors in the current atmospheric temperature profile product. In the TIGR database, we can directly calculate the temperature difference for each atmospheric profile as the bottom level represents the surface. As far as the MOD07/MYD07 product is concerned, we calculate the temperature difference using the temperature at the two lowest effective levels. ATI occurring at higher levels was not considered. The intensity of ATI can be defined as [19], [33]

$$I = \frac{\Delta T}{\Delta H} \times 100 = \frac{T_2 - T_1}{H_2 - H_1} \times 100 \tag{2}$$

where $I$ is the ATI intensity, $T_1$ is the air temperature at the bottom level (surface), and $T_2$ is the air temperature at the top inversion level (unit: K). $H_1$ and $H_2$ are the corresponding altitudes (unit: m).

### C. Evaluation of the Parameterization Scheme Under ATI

As shown in Table I, six widely used parameterization schemes were evaluated in this article. As most of the parameterization schemes are site-specific, their coefficients need to be adjusted using the new representative samples when applied to a new study area. The original coefficients and the coefficients adjusted by Guo *et al.* [17] using globally collected ground measurements are also provided in Table I.

TABLE I
SELECTED CLEAR-SKY PARAMETERIZATION SCHEMES AND THEIR COEFFICIENTS

| Abbreviation of the parameterization scheme | Formula | Original coefficients | Adjusted coefficients |
|---|---|---|---|
| Brunt (1932) | $SDLR = \left(a_1 + b_1 e_a^{1/2}\right)\sigma T_a^4$ | a1=0.52; b1=0.065 | a1=0.6338; b1=0.0426 |
| Swinbank (1963) | $SDLR = \left(a_2 T_a^2\right)\sigma T_a^4$ | a2=9.365*$10^{-6}$ | a2=9.0059*$10^{-6}$ |
| Brutsaert (1975) | $SDLR = \left(a_4 (\frac{e_a}{T_a})^{b4}\right)\sigma T_a^4$ | a4=1.24; b4=1/7 | a4=1.0456; b4=0.0879 |
| Idso (1981) | $SDLR = \left(a_5 + b_5 e_a \exp[\frac{1500}{T_a}]\right)\sigma T_a^4$ | a5=0.7; b5=5.95*$10^{-5}$ | a5=0.6836; b5=4.6869*$10^{-5}$ |
| Prata (1996) | $SDLR = \left(1-[(1+46.5\left(\frac{e_a}{T_a}\right))\exp\left(-\left(a_6 + b_6 46.5\left(\frac{e_a}{T_a}\right)\right)^{1/2}\right)]\right)\sigma T_a^4$ | a5=1.2; b5=3 | a5=1.3471; b5=2.7735 |
| Carmona (2014) | $SDLR = \left(a_7 + b_7 T_a + d_7 Rh\right)\sigma T_a^4$ | a7=-0.34; b7=0.00336; d7=0.00194 | a7=-0.4373; b7=0.0037; d7=0.0027 |

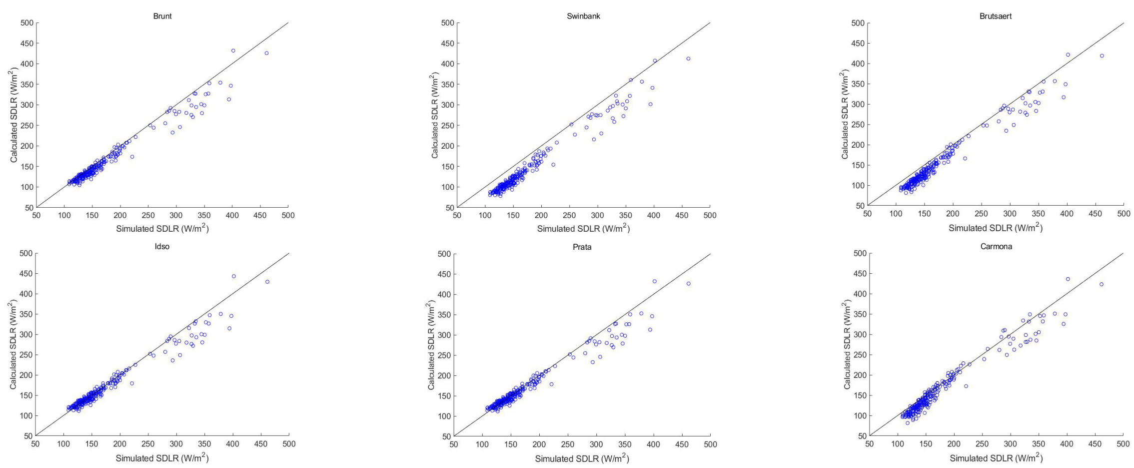


Fig. 2. Comparison of the calculated SDLR and simulated SDLR for the ATI profiles in the TIGR database.

Regarding the TIGR database, we first selected the clear-sky profile. The profiles with a relative humidity greater than 90% at one level or greater than 85% at two successive levels were labeled as cloudy atmospheric profiles and were excluded from the TIGR database [34]. Then, the clear-sky ATI profiles were identified using the temperature profile of the two bottom levels. In total, we obtained 239 clear-sky ATI profiles from the TIGR database. The selected ATI profiles were input into the atmospheric radiative transfer code MODTRAN 5.0 [35] to simulate SDLR. The simulated SDLR was treated as the true value and used to evaluate the SDLR calculated by the selected parameterization schemes. The air temperature and relative humidity at the screen level were linearly interpolated from the two bottom levels of the temperature and water vapor profiles and were used to calculate the SDLR using the equations listed in Table I. When tested by the SURFRAD measurements, the site-measured air temperature and relative humidity were used to calculate the SDLR using the equations listed in Table I, and the site-measured SDLR was treated as the true value. The bias, root-mean-square error (RMSE), and the correlation coefficient ($R$) were used as the primary indicators of the accuracy.

## III. RESULTS

### *A. Evaluation by the TIGR Database*

Fig. 2 shows the evaluation results of the SDLR estimated by the adjusted coefficients using the ATI profiles in the TIGR database. As we can see from Fig. 2, all the parameterization schemes underestimate the SDLR. Furthermore, almost all the parameterization schemes underestimate the SDLR in the range of 250–400 W/m$^2$. The statistical results are provided in Table II. Among the six parameterization schemes, those proposed by Idso [13] and Prata [11] perform better than the other parameterization schemes, with the lowest absolute bias (on the order of 5 W/m$^2$) and RMSE ($\sim$15 W/m$^2$) and the highest determination coefficients (0.97). Followed by Brunt [7] and Carmona *et al.* [9], the absolute

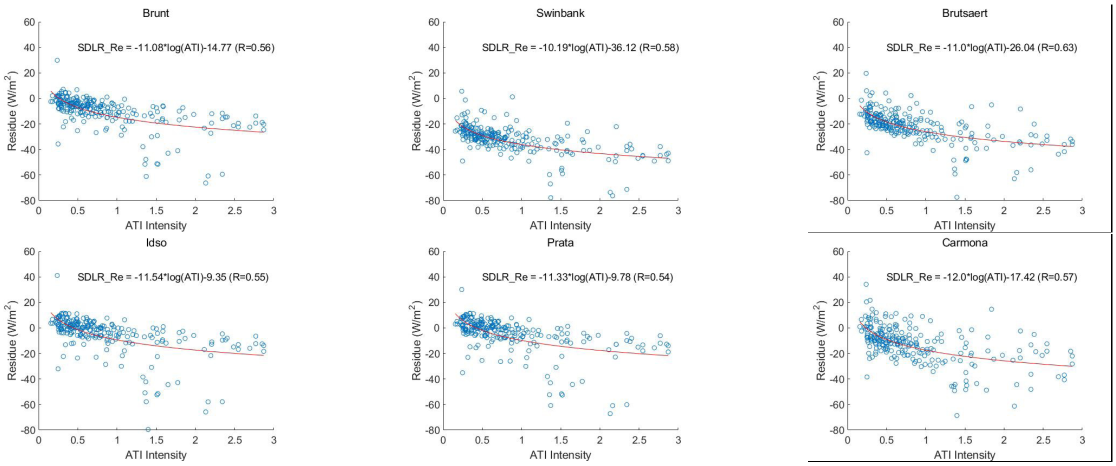


Fig. 3. Scatterplot of the SDLR residuals versus the ATI intensity for the six parameterization schemes.

TABLE II

EVALUATION RESULTS OF THE SIX PARAMETERIZATION SCHEMES FOR ATI AND NORMAL PROFILES IN THE TIGR DATABASE. THE VALUES IN PARENTHESES CORRESPOND TO THE VALUES DERIVED FOR THE NORMAL PROFILES. (UNIT: WATTS PER SQUARE METER)

| Parameterization Scheme | Brunt | Swinbank | Brutsaert | Idso | Prata | Carmona |
|---|---|---|---|---|---|---|
| Bias | -10.32 (4.43) | -32.02 (-8.96) | -21.63 (0.82) | -4.72 (7.69) | -5.23 (6.66) | -12.60 (7.55) |
| RMSE | 24.74 (10.65) | 34.13 (19.15) | 24.74 (11.81) | 15.05 (12.59) | 15.31 (11.94) | 19.14 (15.41) |
| $R^2$ | 0.97 (0.99) | 0.97 (0.97) | 0.97 (0.98) | 0.97 (0.99) | 0.97 (0.99) | 0.95 (0.98) |

bias lies between 10 and 20 W/m$^2$, and the RMSE is less than 24.74 W/m$^2$, and the determination coefficients are larger than 0.95. The parameterization schemes proposed by Swinbank [12] and Brutsaert [10] perform worst.

Using the same method, we investigated the accuracy of the parameterization schemes using normal clear-sky atmospheric profiles (without ATI occurrence) in the TIGR database. We obtained 917 normal profiles. The statistical results are also provided in Table II. The accuracy of the parameterization schemes under normal conditions is similar to that in the study by Guo *et al.* [17], where the absolute bias of each of the six parameterization schemes was less than 5 W/m$^2$. The absolute bias values in this study are all less than 8.96 W/m$^2$. Compared to the performance of the parameterization schemes under normal conditions, the performance of the parameterization schemes in terms of the bias, RMSE, and coefficients of determination under ATI degraded greatly as a whole. As a result, all the parameterization schemes are sensitive to ATI.

Fig. 3 shows the scatterplot between the SDLR residuals (the predicted SDLR minus the simulated SDLR) and the ATI intensity. The SDLR residuals decrease and become more dispersed with increasing ATI intensity. There is a logarithmic relationship between the SDLR residuals and the ATI intensity.

### B. Evaluation by the SURFRAD Data

In total, we extracted 155 clear-sky ATI profiles from three-year MODIS atmospheric profile products at seven SURFRAD sites. The comparison between the calculated SDLR and the site-observed SDLR for the ATI profiles is shown in Fig. 4. Similarly, all the parameterization schemes underestimate the SDLR. The range of the SDLR shown in Fig. 4 is narrower than that shown in Fig. 2. There are only a few samples for which the SDLR exceeds 300 W/m$^2$. The reason lies in that the representativeness of extracted ATI profiles at SURFRAD sites is weaker than that of the ATI profiles extracted from the TIGR database, which causes the representativeness of the samples produced from the SURFRAD sites is slightly worse than the samples produced from the TIGR database. The statistical results are presented in Table III. Among the six parameterization schemes, the performance of the parameterization scheme proposed by Carmona *et al.* [9] is the best, with a bias, RMSE, and determination coefficient of $-4.19$ W/m$^2$, 16.39 W/m$^2$, and 0.89, respectively. The absolute bias, RMSE, and determination coefficients are approximately 15 W/m$^2$, 20 W/m$^2$, and 0.89, respectively, for the parameterization schemes proposed by Brunt [7], Idso (1981), and Prata (1996). The performance of the parameterization schemes proposed by Swinbank [12] and Brutsaert [10] is much worse, with absolute bias and RMSE values larger than 20 and 25 W/m$^2$, respectively. Regarding the different performance of the parameterization schemes for the ATI profiles in the TIGR database and at SURFRAD sites, the reason may be that the ATI profiles at SURFRAD sites are much less representative that those in the TIGR database.

Then, we investigated the performance of the parameterization schemes using normal profiles collocated with six SURFRAD sites. In total, we extracted 4148 normal profiles at the SURFRAD sites. The statistical results are provided in Table III. The absolute bias and RMSE of all the parameterization schemes are less than 6.48 and 14.31 W/m$^2$, respectively, the determination coefficients are larger than 0.94, with the exception of the parameterization scheme proposed by Swinbank [12], whose RMSE is 40.37 W/m$^2$.

In conclusion, the performance of the parameterization schemes in terms of the bias, RMSE, and determination coefficients under ATI degraded greatly when compared to those under normal conditions. All the parameterization schemes are

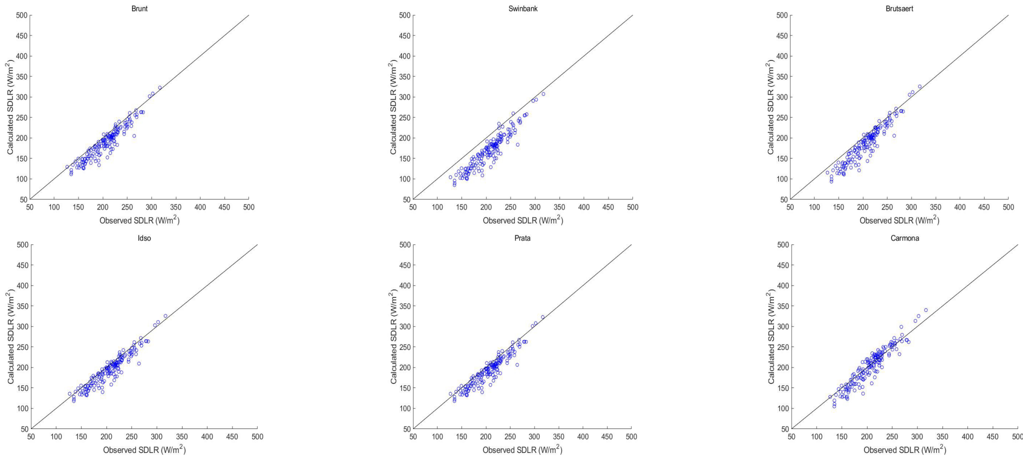


Fig. 4. Comparison of the calculated SDLR and observed SDLR for the ATI profiles at the SURFRAD sites.

TABLE III

EVALUATION RESULTS OF THE SIX PARAMETERIZATION SCHEMES FOR THE ATI AND NORMAL PROFILES AT THE SURFRAD SITES. THE VALUES IN PARENTHESES CORRESPOND TO THE VALUES DERIVED FROM THE NORMAL PROFILES. (UNIT: WATTS PER SQUARE METER)

| Parameterization Scheme | Brunt | Swinbank | Brutsaert | Idso | Prata | Carmona |
|---|---|---|---|---|---|---|
| Bias | -16.89 (2.65) | -37.01 (2.49) | -20.70 (3.99) | -12.16 (2.73) | -13.99 (2.46) | -4.19 (6.48) |
| RMSE | 21.53 (13.16) | 40.37 (27.36) | 25.98 (13.32) | 17.73 (12.33) | 19.01 (13.06) | 16.39 (14.31) |
| $R^2$ | 0.89 (0.94) | 0.88 (0.79) | 0.90 (0.94) | 0.89 (0.95) | 0.89 (0.94) | 0.89 (0.94) |

TABLE IV

EVALUATION RESULTS OF THE SIX PARAMETERIZATION SCHEMES USING THE ORIGINAL COEFFICIENTS FOR THE ATI PROFILES IN THE TIGR DATABASE. (UNIT: WATTS PER SQUARE METER)

| Parameterization Scheme | Brunt | Swinbank | Brutsaert | Idso | Prata | Carmona |
|---|---|---|---|---|---|---|
| Bias | -30.23 | -26.46 | -39.58 | 0.93 | -7.58 | -21.24 |
| RMSE | 33.08 | 29.07 | 41.94 | 13.16 | 15.21 | 25.41 |
| $R^2$ | 0.96 | 0.97 | 0.97 | 0.96 | 0.97 | 0.96 |

sensitive to ATI. We did not find the logarithmic relationship between the SDLR residuals and the ATI intensity at the SURFRAD sites, which may be attributed to the representation of the limited ATI profiles we extracted at SURFRAD sites. The scatterplot is not shown here for simplicity.

## IV. DISCUSSION

### *A. Necessity of Coefficients Adjustment Under ATI*

In Tables II and III, the SDLR was calculated by the coefficients adjusted by the globally distributed ground measurements. The efficacy of coefficient adjustment has been demonstrated by using the observations without specifically considering the occurrence of ATI [9], [17]. In this article, we found that coefficient adjustment can improve the performance of the parameterization schemes under ATI in the TIGR database and SURFRAD sites. For example, the accuracy of the parameterization schemes in terms of the bias and RMSE are improved to some extent with the exception of the parameterization scheme proposed by Idso [13], which can be clearly seen from Tables II and IV.

### *B. Reason for SDLR Underestimation Under ATI*

The physical basis of the parameterization scheme that uses the air temperature and/or water vapor at the screen level to calculate the SDLR is that the SDLR is dominated by the radiation of a shallow layer close to the surface [6]. According to the case study of Gupta, 86% of the SDLR comes from the first layer of the atmosphere, which is 50 hPa thick. We also conducted a sensitivity analysis using an ATI profile in the TIGR database. Fig. 1(a) shows the selected ATI profile, which was input into MODTRAN 5.0 to calculate the contribution of each layer to the total SDLR. As shown in Fig. 1(b), the first layer [from the surface (1013 hPa) to the first level (955 hPa), 58 hPa thick] only accounts for 63.4% of the total SDLR. The reduced contribution of the shallow surface layer to the total SDLR certainly underestimates the SDLR under ATI. The appearance of ATI alters the contribution of the shallow layer near the surface, which violates the assumption of the parameterization scheme and affects the accuracy of the SDLR estimate. This phenomenon is why all the parameterization schemes underestimated the clear-sky SDLR under the ATI profiles (Tables II and III).

### *C. Correct the Impact of ATI*

Current atmospheric profile products such as MODIS [36], Atmospheric Infrared Sounder (AIRS) [36], and Infrared Atmospheric Sounding Interferometer (IASI) [37] are publicly available and can help us identify the occurrence of ATI. With ATI known *a priori*, we can choose a suitable parameterization scheme based on the results of this study and achieve an accurate estimate of the clear-sky SDLR. This is a straightforward approach. How to correct the impact of ATI and improve the accuracy of the parameterization schemes under ATI also deserve trying.

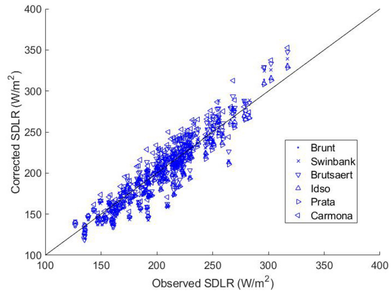


Fig. 5. Comparison between the observed SDLR and the SDLR after correcting the ATI impact.

TABLE V
ACCURACY OF THE SIX PARAMETERIZATION SCHEMES FOR THE ATI PROFILES AT THE SURFRAD SITES AFTER CORRECTING THE ATI IMPACT USING THE FIT LOGARITHMIC FUNCTIONS LIKE (3). (UNIT: WATTS PER SQUARE METER)

| Parameterization Scheme | Brunt | Swinbank | Brutsaert | Idso | Prata | Carmona |
|---|---|---|---|---|---|---|
| Bias | -5.88 | -4.42 | 1.66 | -6.72 | -8.07 | 9.25 |
| RMSE | 14.26 | 15.75 | 15.18 | 14.34 | 15.01 | 18.09 |
| $R^2$ | 0.89 | 0.88 | 0.89 | 0.89 | 0.89 | 0.89 |

According to the scatter plots in Fig. 2, we fit a logarithmic relationship between SDLR residuals and ATI intensity. For example, the formulation between SDLR residuals predicted by Brutsaert [10] can be expressed as

$$\mathrm{SDLR}_{\mathrm{residual}} = -11.0 * \log(\mathrm{ATI}) - 26.04 \tag{3}$$

where $\mathrm{SDLR}_{\mathrm{residual}}$ is the SDLR residuals. We can fit the formulation like (3) to calculate $\mathrm{SDLR}_{\mathrm{residual}}$ for each parameterization scheme, and correct the impact of ATI by minus $\mathrm{SDLR}_{\mathrm{residual}}$ from the estimated SDLR. Fig. 5 shows the comparison between observed SDLR versus the SDLR after correcting the ATI impact at SURFRAD sites. Clearly, most of the points are distributed around the 1:1 line. Table V shows the accuracy of the six parameterization schemes after correcting the ATI impact. Comparing Tables III and V, the performance of parameterization schemes is remarkably improved in terms of the values of bias and RMSEs. The determination coefficients are barely changed. Note the thickness of the ATI layer is different in TIGR database and SURFRAD sites. The difference is not considered in correcting the ATI impact at SURFRAD sites.

## V. CONCLUSION

The occurrence of ATI alters the atmospheric state at the near-surface boundary layer, which substantially affects the accuracy of the clear-sky SDLR estimate. However, no study has investigated the influence of ATI on the estimate of the clear-sky SDLR. This article investigated the impact of ATI on the estimate of the clear-sky SDLR using parameterization schemes. According to the evaluation results using ATI profiles in the TIGR database and SURFRAD sites, all the parameterization schemes are sensitive to ATI, and their accuracy is degraded greatly as a whole. The SDLR is underestimated for ATI profiles from both the TIGR database and SURFRAD sites. The parameterization schemes proposed by Idso [13], Prata [11], and Carmona *et al.* [9] perform better than the other three parameterization schemes, with bias values of approximately $-10$ W/m$^2$ and RMSE values less than 20 W/m$^2$. With the simulation study, we provided the reason for SDLR underestimation for ATI profiles. Finally, we proposed an empirical method to correct the impact of ATI on the estimate of SDLR using the parameterization schemes. The accuracy of all the six parameterization schemes is remarkably improved at SURFRAD sites after correcting the impact of ATI, with the absolute values of bias and RMSEs less than 10 and 20 W/m$^2$ at SURFRAD sites. The development of new parameterization schemes incorporating the impact of ATI is urgently needed.

## ACKNOWLEDGMENT

The MODIS data were obtained from http://reverb.echo.nasa.gov/reverb/ and the SURFRAD data were downloaded from http://www.srrb.noaa.gov

## REFERENCES

[1] S. Liang, K. Wang, X. Zhang, and M. Wild, "Review on estimation of land surface radiation and energy budgets from ground measurement, remote sensing and model simulations," *IEEE J. Sel. Topics Appl. Earth Observat., Remote Sens.*, vol. 3, no. 3, pp. 225–240, Sep. 2010.

[2] J. Cheng and W. Kustas, "Using very high resolution thermal infrared imagery for more accurate determination of the impact of land cover differences on evapotranspiration in an irrigated agricultural area," *Remote Sens.*, vol. 11, no. 6, p. 613, Mar. 2019.

[3] B. R. Barkstrom, "The earth radiation budget experiment (ERBE)," *Bull. Amer. Meteorol. Soc.*, vol. 65, no. 11, pp. 1170–1185, Nov. 1984.

[4] H.-T. Lee and R. G. Ellingson, "Development of a nonlinear statistical method for estimating the downward longwave radiation at the surface from satellite observations," *J. Atmos. Ocean. Technol.*, vol. 19, no. 10, pp. 1500–1515, Oct. 2002.

[5] J. Cheng, S. Liang, and W. Wang, "Surface downward longwave radiation," *Comprehensive Remote Sens.*, S. Liang, Ed. Oxford, U.K.: Elsevier, 2018, pp. 196–216.

[6] J. Schmetz, "Towards a surface radiation climatology: Retrieval of downward irradiances from satellites," *Atmos. Res.*, vol. 23, nos. 3–4, pp. 287–321, Oct. 1989.

[7] D. Brunt, "Notes on radiation in the atmosphere. I," *Quart. J. Roy. Meteorol. Soc.*, vol. 58, no. 247, pp. 389–420, 1932.

[8] A. C. Dilley and D. M. O'Brien, "Estimating downward clear sky long-wave irradiance at the surface from screen temperature and precipitable water," *Quart. J. Roy. Meteorol. Soc.*, vol. 124, no. 549, pp. 1391–1401, 2010.

[9] F. Carmona, R. Rivas, and V. Caselles, "Estimation of daytime downward longwave radiation under clear and cloudy skies conditions over a sub-humid region," *Theor. Appl. Climatol.*, vol. 115, nos. 1–2, pp. 281–295, Jan. 2014.

[10] W. Brutsaert, "On a derivable formula for long-wave radiation from clear skies," *Water Resour. Res.*, vol. 11, no. 5, pp. 742–744, Oct. 1975.

[11] A. J. Prata, "A new long-wave formula for estimating downward clear-sky radiation at the surface," *Quart. J. Roy. Meteorol. Soc.*, vol. 122, no. 533, pp. 1127–1151, 1996.

[12] W. C. Swinbank, "Long-wave radiation from clear skies," *Quart. J. Roy. Meteorol. Soc.*, vol. 90, no. 386, pp. 488–493, Oct. 1964.

[13] S. B. Idso, "A set of equations for full spectrum and 8- to 14-$\mu$m and 10.5- to 12.5-$\mu$m thermal radiation from cloudless skies," *Water Resour. Res.*, vol. 17, no. 2, pp. 295–304, 1981.

[14] S. B. Idso and R. D. Jackson, "Thermal radiation from the atmosphere," *J. Geophys. Res.*, vol. 74, no. 23, pp. 5397–5403, Oct. 1969.

[15] M. Choi, J. M. Jacobs, and W. P. Kustas, "Assessment of clear and cloudy sky parameterizations for daily downwelling longwave radiation over different land surfaces in Florida, USA," *Geophys. Res. Lett.*, vol. 35, no. 20, pp. 288–299, 2008.

[16] J. Cheng, F. Yang, and Y. Guo, "A comparative study of bulk parameterization schemes for estimating cloudy-sky surface downward longwave radiation," *Remote Sens.*, vol. 11, no. 5, p. 528, Mar. 2019.

[17] Y. Guo, J. Cheng, and S. Liang, "Comprehensive assessment of parameterization methods for estimating clear-sky surface downward longwave radiation," *Theor. Appl. Climatol.*, vol. 135, nos. 3–4, pp. 1045–1058, Feb. 2019.

[18] H. Wu, X. Zhang, S. Liang, H. Yang, and G. Zhou, "Estimation of clear-sky land surface longwave radiation from MODIS data products by merging multiple models," *J. Geophys. Res., Atmos.*, vol. 117, no. D22, Nov. 2012, Art. no. D22107, doi: doi:10.1029/2012JD017567.

[19] B.-H. Tang, C. Zhan, Z.-L. Li, H. Wu, and R. Tang, "Estimation of land surface temperature from MODIS data for the atmosphere with air temperature inversion profile," *IEEE J. Sel. Top. Appl. Earth Observ. Remote Sens.*, vol. 10, no. 6, pp. 2976–2983, Jun. 2017.

[20] S. R. Hudson and R. E. Brandt, "A look at the surface-based temperature inversion on the antarctic plateau," *J. Climate*, vol. 18, no. 11, pp. 1673–1696, Jun. 2005.

[21] J.-P. Lagouarde, D. Commandoire, M. Irvine, and D. Garrigou, "Atmospheric boundary-layer turbulence induced surface temperature fluctuations. Implications for TIR remote sensing measurements," *Remote Sens. Environ.*, vol. 138, pp. 189–198, Nov. 2013.

[22] P. J. Minnett, "A numerical study of the effects of anomalous North Atlantic atmospheric conditions on the infrared measurement of sea surface temperature from space," *J. Geophys. Res.*, vol. 91, no. C7, p. 8509, Feb. 2008.

[23] A. Chedin, N. A. Scott, C. Wahiche, and P. Moulinier, "The improved initialization inversion method: A high resolution physical method for temperature retrievals from satellites of the TIROS-N series," *J. Climate Appl. Meteorol.*, vol. 24, no. 2, pp. 128–143, 1985.

[24] Z. Wan and J. Dozier, "A generalized split-window algorithm for retrieving land-surface temperature from space," *IEEE Trans. Geosci. Remote Sens.*, vol. 34, no. 4, pp. 892–905, Jul. 1996.

[25] S. K. Gupta, "A Parameterization for Longwave Surface Radiation from Sun-Synchronous Satellite Data," *J. Climate*, vol. 2, no. 4, pp. 305–320, Apr. 1989.

[26] F. Chevallier, F. Chéruy, N. A. Scott, and A. Chédin, "A neural network approach for a fast and accurate computation of a longwave radiative budget," *J. Appl. Meteorol.*, vol. 37, no. 11, pp. 1385–1397, Nov. 1998.

[27] J. C. Jiménez-Muñoz and J. A. Sobrino, "A generalized single-channel method for retrieving land surface temperature from remote sensing data," *J. Geophys. Res., Atmos.*, vol. 108, no. D22, pp. 2015–2023, 2003.

[28] B. Tang, Y. Bi, Z.-L. Li, and J. Xia, "Generalized split-window algorithm for estimate of land surface temperature from Chinese geostationary FengYun meteorological satellite (FY-2C) data," *Sensors*, vol. 8, no. 2, pp. 933–951, Dec. 2008.

[29] J. Cheng, S. Liang, J. Wang, and X. Li, "A stepwise refining algorithm of temperature and emissivity separation for hyperspectral thermal infrared data," *IEEE Trans. Geosci. Remote Sens.*, vol. 48, no. 3, pp. 1588–1597, Mar. 2010.

[30] B. Tang and Z.-L. Li, "Estimation of instantaneous net surface longwave radiation from MODIS cloud-free data," *Remote Sens. Environ.*, vol. 112, no. 9, pp. 3482–3492, 2008.

[31] J. A. Augustine, J. J. DeLuisi, and C. N. Long, "SURFRAD-A national surface radiation budget network for atmospheric research," *Bull. Amer. Meteorol. Soc.*, vol. 81, no. 10, pp. 2341–2358, 2000.

[32] S. W. Seemann, J. Li, W. P. Menzel, and L. E. Gumley, "Operational retrieval of atmospheric temperature, moisture, and ozone from MODIS infrared radiances," *J. Appl. Meteorol.*, vol. 42, no. 8, pp. 1072–1091, Aug. 2003.

[33] Z. Q. Liu *et al.*, "Temperature inversion characteristics of low-air atmosphere of Urumqi City," *Arid Land Geography*, vol. 30, no. 3, pp. 351–356, 2007.

[34] A. Nie, Q. Liu, and J. Cheng, "Estimating clear-sky land surface longwave upwelling radiation from MODIS data using a hybrid method," *Int. J. Remote Sens.*, vol. 37, no. 8, pp. 1747–1761, Apr. 2016.

[35] A. Berk *et al.*, "MODTRAN 5: A reformulated atmospheric band model with auxiliary species and practical multiple scattering options: Update," *Proc. SPIE*, vol. 5806, pp. 662–667, Jun. 2005.

[36] M. T. Chahine, T. S. Pagano, and H. H. Aumann, "The Atmospheric Infrared Sounder (AIRS): Improving weather forecasting and providing new insights into climate," *Bull. Amer. Meteorol. Soc.*, vol. 87, no. 7, pp. 911–926, 2006.

[37] X. Calbet, P. Schlüssel, T. Hultberg, P. Phillips, and T. August, "Validation of the operational IASI level 2 processor using AIRS and ECMWF data," *Adv. Space Res.*, vol. 37, no. 12, pp. 2299–2305, Jan. 2006.


**Jie Cheng** (Senior Member, IEEE) received the Ph.D. degree in cartography and remote sensing from the Institute of Remote Sensing Applications, Chinese Academy of Sciences, Beijing, China, in 2008.

He was a Post-Doctoral Fellow with the State Key Laboratory of Remote Sensing Science, Beijing Normal University, Beijing, from 2008 to 2010, an Assistant Research Scientist with the University of Maryland, College Park, MD, USA, from 2009 to 2010, and a Visiting Scientist with the Hydrology and Remote Sensing Laboratory, U.S. Department of Agriculture, Agricultural Research Service, Beltsville, MD, USA, from 2017 to 2018. He is currently an Associate Professor with the State Key Laboratory of Remote Sensing Science, Faculty of Geographical Science, Beijing Normal University. His main research interests include estimation of land surface variables from satellite observations, radiative transfer modeling, and studies on surface energy balance.

**Shunlin Liang** (Fellow, IEEE) received the Ph.D. degree from the Boston University, Boston, MA, USA.

He is currently a Professor with the Department of Geographical Sciences, University of Maryland, College Park, MD, USA. He published over 360 SCI indexed peer-reviewed journal articles, 42 book chapters, and 9 special issues of different journals. He authored/edited seven books, four of which were translated in Chinese, such as *Quantitative Remote Sensing of Land Surfaces* (Wiley, 2004), *Advances in Land Remote Sensing: System, Modeling, Inversion and Application* (Springer, 2008), *Advanced Remote Sensing: Terrestrial Information Extraction and Applications* (Academic Press, 2012 and 2019), *Global LAnd Surface Satellite (GLASS) Products: Algorithms, Validation and Analysis* (Springer, 2013), *Land Surface Observation, Modeling, Data Assimilation* (World Scientific, 2013), and *Earth's Energy Budget* (Elsevier, 2017). His main research interests focus on estimation of land surface variables from satellite data, Earth's energy balance, and assessment of environmental changes.

Dr. Liang was the Editor-in-Chief of the nine-volume series *Comprehensive Remote Sensing* (Elsevier, 2017). He was an Associate Editor of the IEEE TRANSACTION ON GEOSCIENCE AND REMOTE SENSING. He is currently an Editor-in-Chief of *Science of Remote Sensing*.

**Jiancheng Shi** (Fellow, IEEE) received the B.S. degree in hydrological geology and geological engineering from the University of Lanzhou, Lanzhou, China, in 1982, and the M.S. and Ph.D. degrees in geography from the University of California at Santa Barbara (UCSB), Santa Barbara, CA, USA, in 1987 and 1991, respectively. He joined the Institute for Computational Earth System Sciences, UCSB, as a Research Professor. He has worked as a PI for more than ten research projects for NASA, five projects for EAS, and four projects for JAXA. In 2010, he became the Director and a Senior Research Scientist with the State Key Laboratory of Remote Sensing Science, sponsored by the Institute of Remote Sensing and Digital Earth, Chinese Academy of Sciences and Beijing Normal University, Beijing, China. He is currently the PI of the Water Cycle Observation Mission (WCOM). He has authored or coauthored more than 200 articles in journals and conferences. His current research interests include microwave remote sensing of water cycle-related components and data assimilation.

Dr. Shi is a fellow of the Electromagnetics Academy and the Society of Photo-Optical Instrumentation Engineers (SPIE).